Spatial correlation properties of the anomalous density matrix in a slab of nuclear matter with realistic NN forces

S. S. Pankratov,[*] E. E. Saperstein,[†] and M. V. Zverev[‡]
Kurchatov Institute, RU-123182 Moscow, Russia

M. Baldo[§]
INFN, Sezione di Catania, 64 Via S.-Sofia, I-95125 Catania, Italy

U. Lombardo[‖]
INFN-LNS and University of Catania, 44 Via S.-Sofia, I-95125 Catania, Italy
(Received 20 October 2008; published 13 February 2009)

Spatial correlation characteristics of the anomalous density matrix $\varkappa$ in a slab of nuclear matter with the Paris and Argonne v_{18} forces are calculated. A detailed comparison with predictions of the effective Gogny force is made. It is found that the two realistic forces lead to very close results that are qualitatively similar to those for the Gogny force. At the same time, the magnitude of $\varkappa$ for realistic forces is essentially smaller than that for the Gogny force. The correlation characteristics are practically independent of the magnitude of $\varkappa$ and turn out to be quite close for the three kinds of forces. In particular, all of them predict a small value of the local correlation length at the surface of the slab and a big one inside. These results are in agreement with those obtained recently by N. Pillet, N. Sandulescu, and P. Schuck [Phys. Rev. C, 76, 024310 (2007)] for finite nuclei with the Gogny force.

DOI: 10.1103/PhysRevC.79.024309 PACS number(s): 21.30.Cb, 21.30.Fe, 21.60.De

I. INTRODUCTION

The problem of the surface nature of nuclear pairing has a long history (see review article Ref. [1] and references therein). First, it was formulated in terms of the effective pairing interaction (EPI) entering the gap equation in a model space in which the pairing problem is usually considered. Within the self-consistent Finite Fermi System theory, the use of a natural density dependent ansatz for the EPI has resulted in a strong attraction at the nuclear surface, being rather small inside nuclei [2]. A similar conclusion was obtained in the *ab initio* calculation of the EPI [3]. Later, the surface enhancement of the gap function $\Delta(X)$ was found by solving the gap equation for the complete Hilbert space in semi-infinite nuclear matter with the realistic Paris force in Ref. [4] and with the effective Gogny force in Ref. [5]. Similar conclusions were obtained for a nuclear slab in Ref. [6] where the gap equation was solved for both types of NN force simultaneously. It was found that, although there is a quantitative difference between the predictions of the two calculations, both of them show a pronounced maximum of $\Delta(X)$ at the surface of the slab, $X = L$, where $2L$ is the slab width, the effect being stronger for smaller values of L. In more detail, the gap equation for the nuclear slab was solved in Ref. [7] for the Paris force and in Ref. [8] for the Argonne v_{18} force. It turned out that predictions of these two absolutely different kinds of realistic NN force for the gap function agree with each other within 10%, both yielding the ratio $\Delta(X \simeq L)/\Delta(X = 0) \simeq 2$.

Recently, Pillet, Sandulescu, and Schuck [9] investigated directly spatial properties of the anomalous density $\varkappa$, which determines the space distribution of Cooper pairs. Calculations were carried out within the Hartree-Fock-Bogoliubov (HFB) approach by employing the D1S Gogny interaction [10] for a set of Sn, Ni, and Ca isotopes. It was shown that Cooper pairs in nuclei preferentially are located with small size (2–3 fm) in the surface region. The relevance of this phenomenon to two-nucleon transfer reactions was discussed. It should be mentioned that earlier the correlation properties of pairing for specific nuclei were studied by Catara *et al.* [11], Ferreira *et al.* [12], Bertsch and Esbensen [13], and Hagino *et al.* [14] and in several works cited in Ref. [9]. A similar investigation has also been performed for $T = 0$ pairing in dilute nuclear matter [15].

In this article we carry out an analogous study for a nuclear slab with realistic NN force (the Paris and Argonne v_{18} potentials) and the Gogny force. Our goal is to compare predictions for the correlation pairing characteristics of the Gogny force and of realistic forces to analyze to what extent the effect found in Ref. [9] is general and independent on the specific choice of NN force. It should be mentioned that, with small modifications, the nuclear slab configuration may be used to describe the so-called "lasagna" phase of the inner crust of neutron stars.

II. MAIN DEFINITIONS

To make the comparison easier, let us recall the main definitions introduced in Ref. [9]. In a inhomogeneous system,

[*]pankratov@mbslab.kiae.ru
[†]saper@mbslab.kiae.ru
[‡]zverev@mbslab.kiae.ru
[§]baldo@ct.infn.it
[‖]lombardo@lns.infn.it

the anomalous density matrix is defined as follows:

$$\varkappa(\mathbf{r}_1,\mathbf{r}_2) = \sum_i u_i(\mathbf{r}_1)v_i(\mathbf{r}_2), \tag{1}$$

where $u_i(\mathbf{r})$, $v_i(\mathbf{r})$ are the Bogolyubov functions. For a spherical nucleus, it is convenient to go to relative and center of mass coordinates, $\mathbf{r} = \mathbf{r}_1 - \mathbf{r}_2$ and $\mathbf{R} = (\mathbf{r}_1 + \mathbf{r}_2)/2$. In Ref. [9] the anomalous density matrix was studied in such a way that the probability distribution of Cooper pairs, $|\varkappa(\mathbf{R},\mathbf{r})|^2$, was averaged over the angle between the vectors $\mathbf{R}$ and $\mathbf{r}$,

$$\varkappa^2(R,r) = \frac{1}{4\pi}\int |\varkappa(\mathbf{R},\mathbf{r})|^2\, d\Omega\ . \tag{2}$$

In particular, the space distribution of the pairing tensor $|\varkappa(R,r)|^2$ was analyzed. The probability distribution of pairing correlations,

$$P(R,r) = R^2 r^2 \varkappa^2(R,r), \tag{3}$$

was calculated in Ref. [9]. To avoid misunderstanding, this quantity is not normalized to unity.

The coordinate dependent local correlation length was defined as

$$\xi(R) = \frac{(\int r^2\varkappa^2(R;r)\, d^3r)^{1/2}}{(\int \varkappa^2(R;r)\, d^3r)^{1/2}}\ . \tag{4}$$

At last, the locally normalized pairing tensor was considered in the form

$$W(R,r) = \frac{r^2\varkappa^2(R,r)}{\int \varkappa^2(R,r)\, r^2 dr}, \tag{5}$$

because it enters the definition of the correlation length.

Just as in Ref. [8], we consider a nuclear slab embedded into the Saxon-Woods potential $U(x)$ symmetrical with respect to the point $x = 0$ with potential well depth $U_0 = -50$ MeV and diffuseness parameter of $d = 0.65$ fm typical for finite nuclei. The chemical potential is taken equal to $\mu = -8$ MeV. To compare our calculations with those of Ref. [9], we fixed the thickness parameter of the slab as $L = 6$ fm to mimic nuclei of the tin region. We use the notation $\mathbf{r} = (\mathbf{s},x)$, where $\mathbf{s}$ is the two-dimensional vector in the plane perpendicular to the x axis. The system under consideration is homogeneous in the $\mathbf{s}$ plane; therefore one has $\varkappa(\mathbf{r}_1,\mathbf{r}_2) \to \varkappa(\mathbf{R},\mathbf{r}) \to \varkappa(X;x,\mathbf{s})$, with the obvious notation. The definition (4) is then rewritten as follows:

$$\xi^2(X) = \frac{\int (x^2+s^2)|\varkappa(X;x,\mathbf{s})|^2\, d^3r}{\int |\varkappa(X;x,\mathbf{s})|^2\, d^3r}\ . \tag{6}$$

As far as the correlation properties in the x direction and in the $\mathbf{s}$ plane are essentially different, it looks reasonable to consider them separately,

$$\xi^2(X) = \xi_x^2(X) + \xi_s^2(X), \tag{7}$$

with the obvious notation.

In the slab geometry, the angular averaging procedure similar to that in Eq. (2) is as follows:

$$\varkappa^2(X,r) = \frac{1}{4\pi}\int |\varkappa(X;x,\mathbf{s})|^2\, \frac{2}{r}\, \delta(r^2 - x^2 - s^2)\, d^2s\, dx. \tag{8}$$

It gives the distribution of the pairing tensor for a fixed value of the three-dimensional relative distance r. There is another possibility, just to integrate over $\mathbf{s}$:

$$\varkappa^2(X,x) = \int |\varkappa(X;x,\mathbf{s})|^2\, d^2s\ . \tag{9}$$

It yields the quantity $\varkappa^2(X,x)$ which gives the distribution of the pairing tensor in variables which are natural for a slab. For brevity, we use the same notation for the integrated anomalous density matrix as for the initial one and the one in Eq. (8). The arguments should help to avoid misleading. Note that $\varkappa(X,x)$ and $\varkappa(X,r)$ have different dimensions.

III. CALCULATION RESULTS

Methods of solving the gap equation and the Bogolyubov equations for a nuclear slab are described in Ref. [7] for the separable representation of the Paris potential and in Ref. [8] for the Argonne v_{18} force. The latter could be used for arbitrary NN potential, and we repeated all the calculations of Ref. [8] for the Gogny force. To begin the comparison, let us start from infinite nuclear matter. The dependence of the gap on the density of nuclear matter for the three kinds of NN force is displayed in Fig. 1. The correlation length (4) in infinite matter can be easily found in the momentum space:

$$\xi^2 = \frac{\int \left|\frac{\partial}{\partial k}\varkappa(k)\right|^2 d^3k}{\int |\varkappa(k)|^2 d^3k}. \tag{10}$$

Let us substitute in this equation $\varkappa(k) = \Delta(k)/2E_k$, where $E_k = \sqrt{(\varepsilon_k - \varepsilon_F)^2 + \Delta^2(k)}$, $\varepsilon_k = k^2/2m^*$, and $\varepsilon_F = k_F^2/2m^*$. The functions inside the integrals both in the numerator and in the denominator of this relation are very peaked in the vicinity of $k = k_F$ and rapidly vanish outside the interval $|k - k_F| \lesssim k_F(\Delta_F/\varepsilon_F)$, $\Delta_F = \Delta(k_F)$. Usually one deals with the limit $(\Delta_F/\varepsilon_F) \ll 1$. In this case, one can substitute $\Delta(k) = \Delta_F$ in Eq. (10) and evaluate the integrals analytically. A simple calculation yields

$$\xi = \frac{v_F}{\sqrt{8}\Delta_F}, \tag{11}$$

where $v_F = k_F/m^*$.

The correlation length for the three kinds of force under discussion found numerically from Eq. (10), with $m^* = m$,

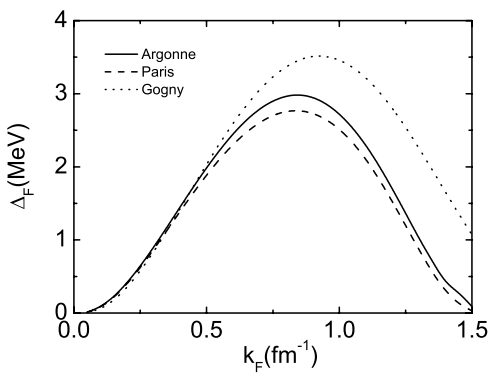

FIG. 1. The gap $\Delta(k = k_F)$ in infinite nuclear matter.

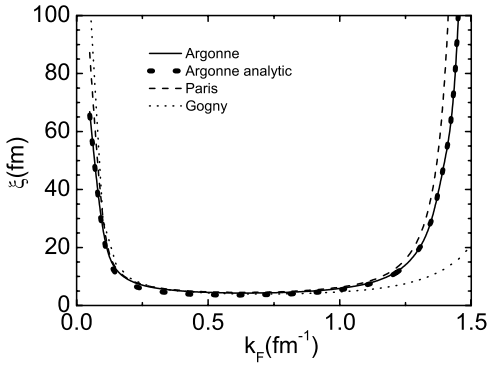

FIG. 2. The correlation pairing length in infinite nuclear matter.

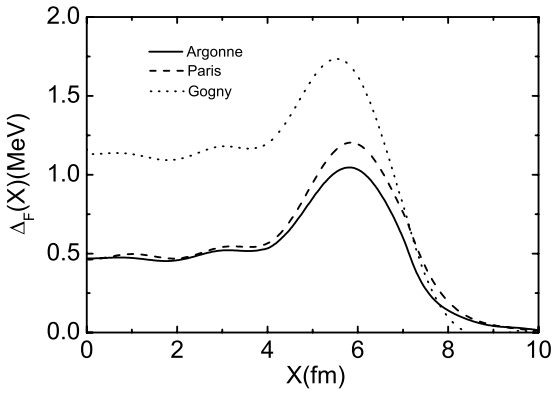

FIG. 3. The Fermi averaged gap $\Delta_F(X)$.

are displayed in Fig. 2. For comparison, the approximate ξ from Eq. (11) with Argonne force is also displayed. It is seen that the approximate formula works sufficiently well in all the interval of k_F. Even at the maximum of the gap the deviation from the numerical result is of the order of 15%.

One can see that at small density, $k_F < 0.5$ fm^{-1}, the results for all three forces practically coincide. This is not strange. Indeed, although the Gogny force is an effective one, in the $^1S_0$ channel under consideration it describes the free NN scattering perfectly well for small energy values that are only important in this density interval. In this sense, the Gogny force could be considered as a semirealistic force. Two realistic forces lead to close results for all density values. In the vicinity of the gap maximum, the difference between $\Delta^{\rm Arg}$ and $\Delta^{\rm Par}$ does not exceed 10%, and only at $k_F \simeq 1.4$ fm^{-1}, where the gap value itself becomes very small, does the relative difference become larger. As to the Gogny force, at the density region $k_F \simeq 1$ fm^{-1} it leads to the gap values that are bigger by approximately $(20 \div 30)$% than those for realistic forces. Correspondingly, the correlation length for the Gogny force is quite close to that of the realistic forces till $k_F \simeq 0.8$ fm^{-1}, and only at $k_F \simeq 1.2$ fm^{-1} does the difference become large. The density dependence of the correlation length, $\xi(k_F)$, is qualitatively similar for all the three types of force. It consists of a plateau at $0.3 \lesssim k_F \lesssim 1$ fm^{-1} and two intervals of sharp growth, at $k_F \lesssim 0.3$ fm^{-1} and $k_F \gtrsim 1$ fm^{-1}. In the latter, the value of $\xi^{\rm Gog}(k_F)$ is growing with k_F much slower than that of $\xi^{\rm Arg}(k_F)$ and $\xi^{\rm Par}(k_F)$. Note that at $k_F \gtrsim 1.2$ fm^{-1} the difference between $\xi^{\rm Arg}(k_F)$ and $\xi^{\rm Par}(k_F)$ also becomes noticeable. This is a manifestation of their behavior near the critical point k_F^c at which the gap vanishes and transition to the normal phase of nuclear matter occurs. The values of k_F^c for the Argonne force and the Paris potential are a little different. This results in different behavior of $\xi^{\rm Arg}(k_F)$ and $\xi^{\rm Par}(k_F)$ in the region of $k_F \simeq 1.5$ fm^{-1}.

Let us now turn to the slab system. Before analyzing the correlation characteristics, it is instructive to briefly compare the EPI and the gap itself found with the realistic forces and the Gogny force. The "Fermi averaged" gap is displayed in Fig. 3. It is defined as

$$\Delta_F(X) = \Delta(X, k_F(X)), \tag{12}$$

where the local Fermi momentum is $k_F(X) = \sqrt{2m(\mu - U(X))}\ \Theta(\mu - U(X))$. This quantity characterizes the gap on average [1,7,8]. We see, first, that all three functions $\Delta_F(X)$ have pronounced maxima at $X \simeq L = 6$ fm. The ratio $\Delta_F(X \simeq L)/\Delta_F(X = 0) \simeq 2$ for realistic forces and $\simeq 1.5$ for the Gogny force, in agreement with Ref. [6]. Second, the gap $\Delta_F^{\rm Gog}$ is significantly bigger than $\Delta_F^{\rm Par}$ and $\Delta_F^{\rm Arg}$, by approximately a factor of one and a half at the surface and two inside the slab. It is worth discussing this point in more detail. Let us consider ^{120}Sn as a "reference nucleus." Its empirical gap value is estimated usually as $\Delta \simeq 1.3$ MeV [16,17]. Diagonal matrix elements of the gap found in Refs. [7] and [8] for a slab with $L = 6$ fm are about 1 MeV, which agrees with the above value, leaving about 20–30% for the surface vibration contribution. The latter was estimated in Ref. [17] as $\simeq$50%, which is, in our opinion, too much (see discussion in Ref. [1]). We consider the estimation of Ref. [18] at $\simeq$30% as more realistic, but, evidently, also too big, because of disregarding so-called tadpole diagrams [19]. Calculations of Ref. [9] for this nucleus gave $\Delta \simeq 2$ MeV, which, in our opinion, is too much, especially if you take into account what the additional contribution of surface vibrations to the mean field theory value of Δ will be! Thus, our observation in slab calculations that the Gogny force overestimates the gap value agrees essentially with the results of Ref. [9].

To understand the physical reason for the surface enhancement of the pairing gap with each NN force under consideration and the bigger values of the gap for the Gogny force, it is useful to calculate the EPI that we use in the two-step method of solving the gap equation [1]. Let us review how this quantity is defined. In a symbolic form, the microscopic gap equation reads

$$\Delta = \mathcal{V} A^s \Delta, \tag{13}$$

where $\mathcal{V}$ is the free NN potential and $A^s = GG^s$ stands for the two-particle propagator in the superfluid system. Here G and G^s are the one-particle Green functions without and with pairing effects taken into account, respectively. In Eq. (13), as usual, integration over intermediate coordinates and summation over spin variables is understood. Let us now split the complete Hilbert space S of two-particle states into two parts, $S = S_0 + S'$. The first one is the model subspace S_0 in which the gap equation is considered, and the other is the complementary subspace S'. They are separated by the energy E_0 in such a way that S_0 involves all the two-particle

states (λ,λ') with the single-particle energies $\varepsilon_\lambda, \varepsilon_{\lambda'} < E_0$. The complementary subspace S' involves the two-particle states for which one of the energies ε_λ, $\varepsilon_{\lambda'}$ or both of them are greater than E_0. Therefore, pairing effects can be neglected in S' if E_0 is sufficiently large. The validity of inequality $\Delta^2/(E_0-\mu)^2 \ll 1$ is the criterium of such an approximation. Correspondingly, the two-particle propagator is represented as the sum $A^s = A^s_0 + A'$. Here we already neglected the superfluid effects in the S' subspace and omitted the superscript "s" in the second term. The gap equation (13) can be rewritten in the model subspace,

$$\Delta = V^p_{\rm eff}\, A^s_0\, \Delta, \tag{14}$$

where the EPI should be found in the supplementary subspace,

$$V^p_{\rm eff} = \mathcal{V} + \mathcal{V} A'\, V^p_{\rm eff}. \tag{15}$$

Note that the last equation has a strong similarity with the Bethe-Goldstone equation.

As the analysis showed [7,8], the optimal choice of splitting corresponds to $E_0 = 15 \div 20$ MeV. In a slab system, the EPI is calculated in the mixed coordinate-momentum representation [1]. To illustrate graphically properties of the EPI, we present it in a localized form [7,8] with the Fermi averaged strength

$$\mathcal{V}^{\rm F}_{\rm eff}(X) = \int dt\, V^p_{\rm eff}\left(k_1 = k_2 = k_{\rm F}(X); X + \frac{t}{2}, X - \frac{t}{2}\right). \tag{16}$$

The Fermi averaged EPI for the Argonne v_{18} force and the Gogny D1S force calculated for $E_0 = 15$ MeV are displayed in Fig. 4. We did not display the EPI for the Paris potential as it practically coincides with that for the Argonne force. One can see that both the curves behave in a similar way changing from a quite weak attraction inside the slab to a very strong attraction outside. The reason for the latter is that in the asymptotic region $X > L$ the $\mathcal{V}^{\rm F}_{\rm eff}$ value tends to the quantity that is very close to the free T matrix taken at the negative energy $E = 2\mu$. To be precise, the limit is equal to $T(E = 2\mu)$ if the separating energy $E_0 = 0$. In the case of $E_0 \neq 0$ the limit is equal to some "T' matrix" that is obtained by solving the same Lippman-Schwinger equation as the T matrix, but in a cut momentum space, because the contribution of nucleons with total energy less than E_0 must be pulled out. As it is known, the Gogny force leads to the scattering length in the $^1S_0$ channel $a \simeq 12$ fm [13,14]. It differs, of course, from the experimental value of $a \simeq 18$ fm that is reproduced by any realistic force, but not so much. In any case, the virtual pole of the T matrix for the Gogny force is close to zero as it should be. Therefore the analytical continuation of the T matrix (or T' matrix) to rather small negative energy $E = 2\mu$ results in an enhancement of the T' matrix ($\simeq -950$ MeV fm^3) in comparison with typical values. This enhancement is not so strong as in the case of the Argonne force ($\simeq -1100$ MeV fm^3), but it is equally significant. The inner value of the EPI for the Gogny force is quite small ($\simeq -160$ MeV fm^3), but is bigger than that for the Argonne one ($\simeq -95$ MeV fm^3). In our previous study with realistic forces [1,7,8] we explained the surface enhancement of the gap in terms of the sharp variation of the EPI at the surface. In the case of the Argonne force, the ratio $\mathcal{V}^{\rm out}_{\rm eff}/\mathcal{V}^{\rm in}_{\rm eff} \simeq 12$. For the Gogny force, it is about 6. This is also a big number leading to a surface enhancement of the gap, but not so pronounced as for realistic force. Figure 4 explains also why the Gogny gap is so big. It is well known that the pairing gap depends on the interaction strength in an exponential way. In Ref. [7] it was found that 1% variation of $\mathcal{V}^{\rm in}_{\rm eff}$ leads to 5% variation of the gap. It explains why the gap function for the Gogny force is $1.5 \div 2$ times greater than the one for realistic forces.

Let us turn now to the correlation pairing characteristics. The total correlation lengths ξ and the correlation lengths in x direction ξ_x found from Eq. (7) for each kind of force are displayed in Figs. 5 and 6, respectively. The curve $\xi^{\rm Arg}(X)$ is quite similar to $\xi^{\rm Par}(X)$, the difference is about 5%. Both have a minimum shifted a little from the surface, $X = L$, in the direction of the free space, both have a pronounced maximum in the vicinity of $X = 0$ and grow rapidly to the right from the minimum. Qualitatively, the curve $\xi^{\rm Gog}(X)$ behaves in a similar way, but the maximum value at $X = 0$ is approximately two times less than the values for realistic forces. The minimum of $\xi^{\rm Gog}(X)$ is also shifted from the point $X = L$, but the value of the shift is less. Such a behavior of each curve $\xi(X)$ qualitatively agrees with naive local density approximation (LDA) predictions. Indeed, inside the slab, the local Fermi momentum $k_{\rm F}(X \simeq 0) \simeq \sqrt{2m(\mu - U_0)} \simeq 1.4$ fm^{-1}, which corresponds to big values of ξ in infinite matter (see Fig. 2). The same is true at $X > 8$ fm where the local Fermi momentum

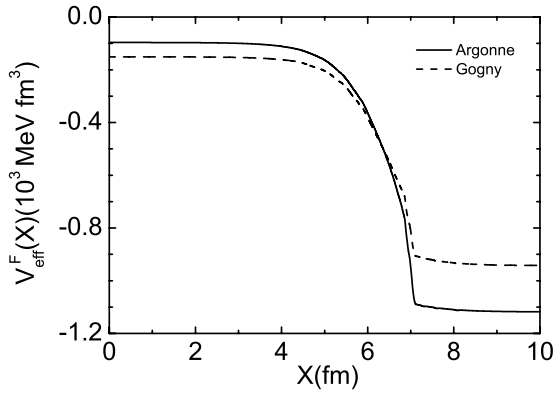

FIG. 4. The Fermi averaged effective pairing interaction $\mathcal{V}^{\rm F}_{\rm eff}(X)$.

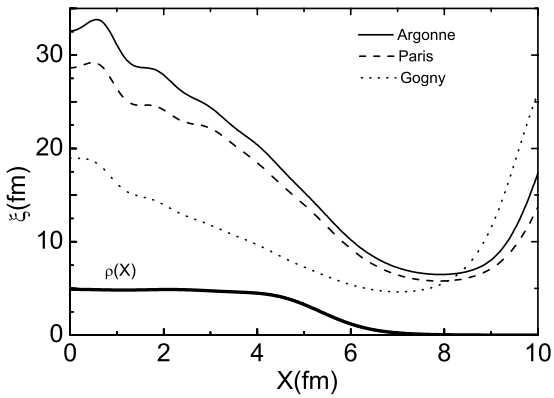

FIG. 5. The correlation pairing length $\xi(X)$ in a slab of nuclear matter.

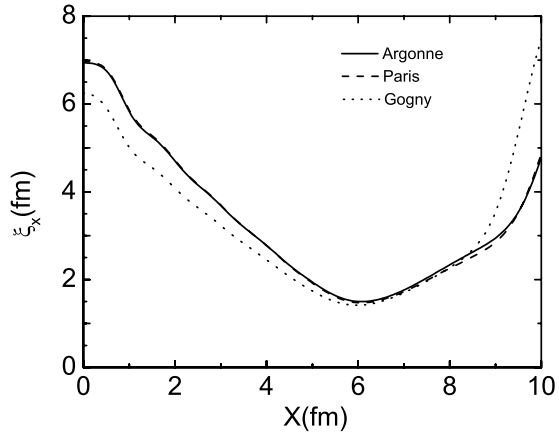

FIG. 6. The correlation pairing length $\xi_x(X)$ in the x direction for a slab of nuclear matter.

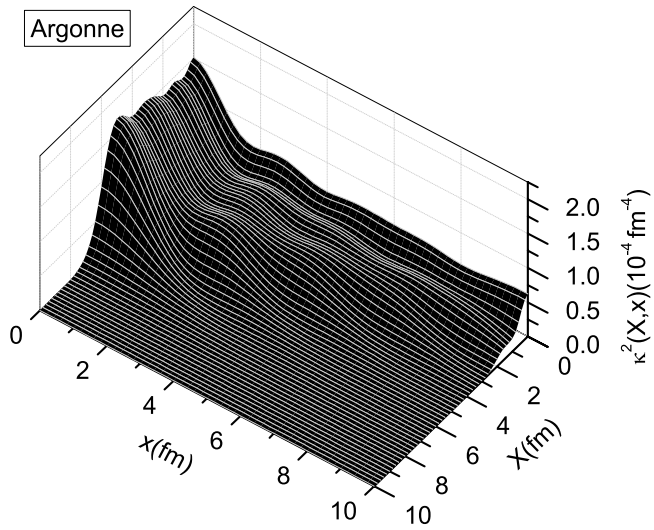

FIG. 7. The pairing tensor distribution $\varkappa^2(X,x)$.

vanishes. But under more detailed examination, deviations from the LDA predictions are significant. To illustrate this point, we show in Fig. 5 with a thick line, in arbitrary units, the density distribution $\rho(X)$. Within the LDA, the correlation length $\xi(X)$ should show a plateau inside the slab, just as the density does. Instead, $\xi(X)$ is decreasing rapidly with the increase of X till $X \simeq L$. Qualitatively, the coordinate dependence of the function $\xi(X)$ in the slab reminds us of that of $\xi(R)$ in spherical nuclei found in Ref. [9]. Both of them have minima at the surface region and pronounced maxima in the center. But any quantitative comparison is hardly possible because, for the problem under consideration, the properties of the two systems are essentially different. Indeed, in a spherical nucleus all particles move in a finite space limited by the nuclear surface. In contrast, in a slab the particle motion is limited only in the x direction. In the **s** plane, the motion is free, which leads to very big values of ξ_s in Eq. (7) and ξ close to that in the infinite system. As to the $\xi_x(X)$ function, it should be much closer to $\xi(R)$ of Ref. [9]. As it is seen in Fig. 6, the two curves $\xi_x^{\rm Arg}(X)$ and $\xi_x^{\rm Par}(X)$ practically coincide. Deviation of $\xi_x^{\rm Gog}(X)$ from both is much less than in the case of the total correlation length. It doesn't exceed 15%. All three curves have a common minimum at $X \simeq L$, with the value of $\xi_x^{\rm min} \simeq 1.5$ fm. It is not far from the value of $\xi^{\rm min} \simeq 2$ fm found in Ref. [9] for Sn isotopes. Evidently, the difference is mainly due to geometry effects. Thus, for a nuclear slab, the correlation length of pairing in the x direction at the surface, calculated with realistic and semirealistic Gogny forces, is very small, in agreement with the conclusions of Ref. [9].

To visualize the pairing tensor distribution, we draw a three-dimensional plot in Fig. 7 for the $\varkappa^2(X,x)$ function given by Eq. (9) for the Argonne force. We see that there is a set of maxima at $x = 0$, the highest one being near to the slab surface, $X \simeq L$. Figure 8 shows the profile functions $\varkappa^2(X = X_0,x)$ for several values of X_0 corresponding to the maximum positions. The nearest to the surface maximum is at $X_0 \simeq 5$ fm, the neighboring one is at $X_0 \simeq 3$ fm. There is also a pronounced maximum at $X_0 = 0$. The surface peak is very narrow, in correspondence with Fig. 6. On the contrary, in the case of $X_0 = 0$ a comparatively sharp peak is accompanied by a flat base plate which results in a big value of ξ_x. The similar profile functions are drawn, in the same figure, for the Paris and Gogny forces. The Paris curves are again quite similar to the Argonne ones. As to the Gogny force, the similarity takes place only at a qualitative level, absolute values of $\varkappa^2$ being bigger than those for realistic forces. This is the result of bigger values of the gap itself for the Gogny force, as illustrated in Fig. 3. We see that $\Delta_{\rm F}^{\rm Par}$ is a little bigger than $\Delta_{\rm F}^{\rm Arg}$; therefore $(\varkappa^{\rm Par})^2$ is, on average, bigger than $(\varkappa^{\rm Arg})^2$. On the other side, $\Delta_{\rm F}^{\rm Gog}$ is significantly bigger than the gap for realistic forces. As a result, $(\varkappa^{\rm Gog})^2$ significantly exceeds the microscopic values as well. Note that the correlation length $\xi(X)$, Eq. (6), does not depend on the magnitude of $\varkappa$, giving rise to a much smaller difference between the Gogny and realistic forces. The same is true for $\xi_x(X)$, Eq. (7). The surface peak dominates, to some

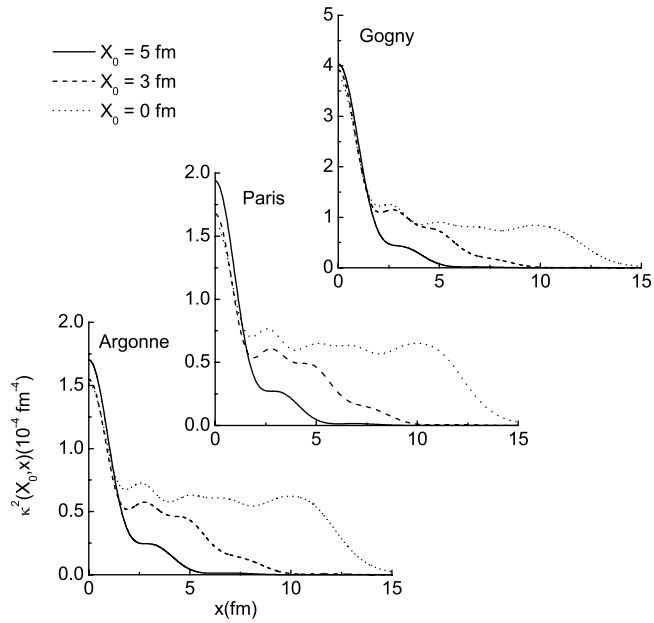

FIG. 8. The profile functions $\varkappa^2(X = X_0,x)$.

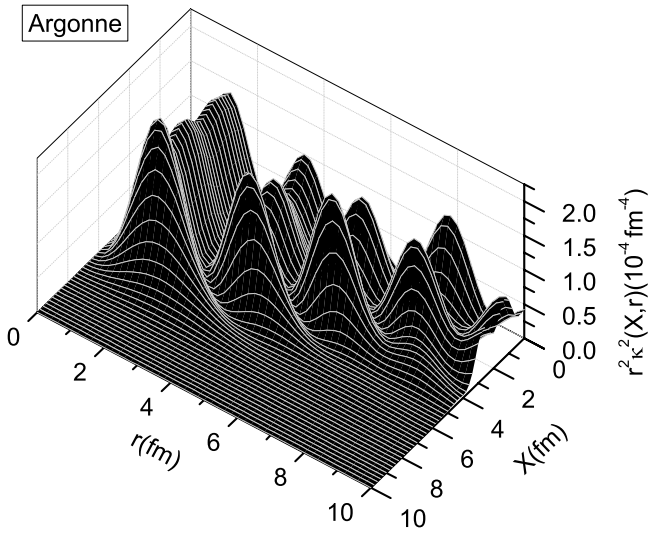

FIG. 9. The probability distribution $r^2\varkappa^2(X,r)$.

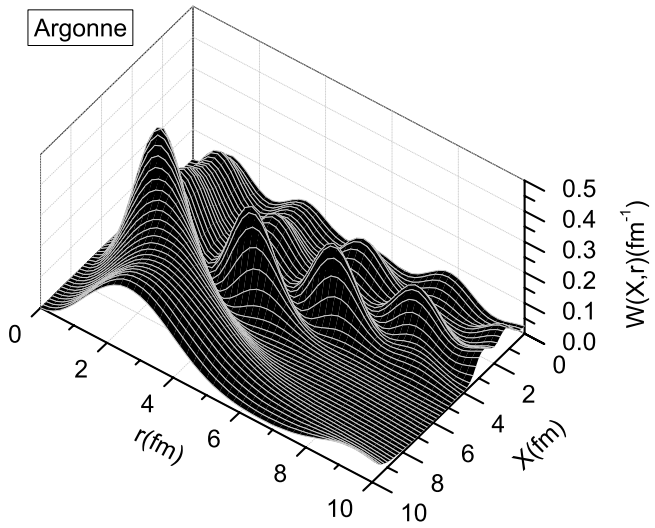

FIG. 11. The locally normalized pairing tensor $W(X,r)$.

extent, for all three kinds of forces, and this effect for realistic forces is even stronger than that for the Gogny force.

The $\varkappa^2(X,r)$ function given by Eq. (8) multiplied by r^2 gives the probability distribution of pairing correlations similar to Eq. (3) in the case of the spherical symmetry. It is displayed in Fig. 9, again for the Argonne force. Now the main maximum positions are shifted from $r = 0$ to $r \simeq 1 \div 2$ fm due to the factor r^2. The surface maximum at $X \simeq L$ is even more pronounced than in Fig. 7. To compare results obtained for the different forces under consideration, we again draw the profile functions $r^2\varkappa^2(X = X_0,r)$ (see Fig. 10). Again, just as in Fig. 8, the Gogny force results are significantly bigger than those of the realistic ones in magnitude but are very similar in form. Again the surface maxima dominates and again the surface enhancement is stronger for realistic forces.

To make the comparison with Ref. [9] more complete, we display in Fig. 11 the locally normalized pairing tensor, which is defined as

$$W(X,r) = \frac{r^2\varkappa^2(X,r)}{\int \varkappa^2(X,r)\, d^3r}, \tag{17}$$

similar to the definition (5) in spherical systems. The profile functions $W(X = X_0,r)$ are displayed in Fig. 12, which is analogous to Figs. 8 and 10. In this case, the Gogny force curves are close to those for realistic forces not only in form but also in magnitude. This happens because the $\varkappa^2$ quantity appears in both the numerator and the denominator of Eq. (17), the result being almost independent of the magnitude of $\varkappa$. An absolutely similar situation occurs with calculations of the correlation lengths ξ and ξ_x.

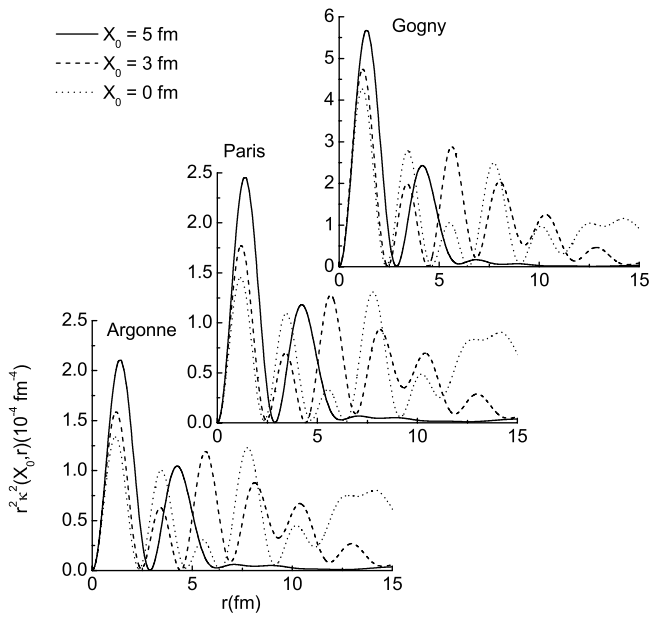

FIG. 10. The profile functions $r^2\varkappa^2(X = X_0,r)$.

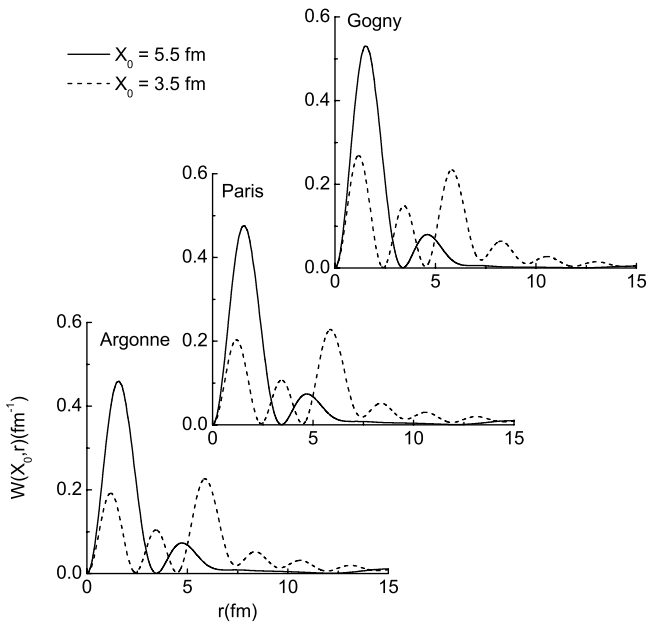

FIG. 12. The profile functions $W(X_0,r)$.

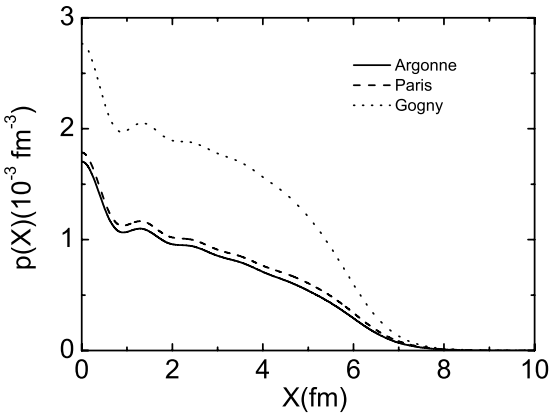

FIG. 13. The integrated Cooper pair probability distribution $p(X)$.

The denominator of Eq. (17),

$$p(X) = \int \varkappa^2(X,r)\, d^3r = \int \varkappa^2(X,x)\, dx, \qquad (18)$$

gives the total probability distribution of Cooper pairs integrated over relative coordinates. Note that this quantity displayed in Fig. 13, like $P(R,r)$ in Eq. (3), is not normalized to unity. Again we see that the result for the Gogny force behaves qualitatively similar to those for the realistic forces but its magnitude is significantly bigger. And for each force under consideration this quantity in the slab does not exhibit any surface enhancement. It occurred because, although the surface maximum for any force in Fig. 8 is higher than the central one, the correlation length in the x direction at the surface is much smaller than that inside the slab, which makes the integral over x smaller. An analogous effect should take place in nuclei, too, but in this case the "geometrical" factor R^2 in Eq. (3) would help the surviving of the surface enhancement in the Cooper pair distribution if the probability $P(R,r)$, Eq. (3), were integrated over the relative coordinates.

IV. CONCLUSION

Spatial correlation properties of nuclear pairing in a nuclear slab are studied with two realistic NN potentials, the Paris and Argonne v_{18}, and with the phenomenological Gogny D1S interaction. The results obtained with the two realistic forces agree with each other with an accuracy of about 10%. But they agree only qualitatively with those of the Gogny force. The gap value in the slab for the Gogny force exceeds that from the realistic forces by a factor about 2, which results in rather bigger values of the anomalous density matrix $\varkappa$. Nevertheless, some of main conclusions of Ref. [9] obtained for finite nuclei with the Gogny force are confirmed qualitatively, especially the dependence of the correlation length on the position of the c.m. of a Cooper pair. This quantity does not depend practically on the absolute value of $\varkappa$, only the space distribution of the pairing tensor $\varkappa^2(X,x)$ being important. At the surface of the slab the local value of the correlation length in the x direction is very small, $\xi_x(X \simeq L) \simeq 1.5$ fm, for all three kinds of force under consideration. Inside the slab ξ_x becomes very large, i.e., of the order of the slab width or even more. Thus, on this point our results completely confirm those of Ref. [9].

The pairing tensor $\varkappa^2(X,x=0)$ has several maxima, among them the ones at $X = 0$ and $X \simeq L$ are most pronounced. And the one at the surface is a bit higher, especially for realistic forces. In this sense, we can speak of surface enhancement of the Cooper pair distribution. However, the total probability $p(X)$ for a pair to have the c.m. coordinate X, which is obtained by integrating $\varkappa^2(X,x)$ over relative coordinate, has no surface enhancement. Thus, the second conclusion of Ref. [9] that Cooper pairs in nuclei prefer to be concentrated in the vicinity of the surface should not be drawn for a slab. We explain this with different geometrical properties of two systems under comparison, with different "surface-to-volume ratio" in a sphere and in a slab. However, all surface enhancement features found for realistic forces are qualitatively reproduced with the Gogny force. We trace this effect to the "semirealistic" nature of the Gogny force, which describes the low-energy NN scattering in the $^1S_0$ channel sufficiently well. It seems reasonable to suppose that all the main conclusions of Ref. [9] will be confirmed qualitatively if the Gogny force in the pairing channel is replaced by a realistic NN potential.

ACKNOWLEDGMENTS

Two of us (S.P. and E.S.) thank the INFN, Seczione di Catania, for hospitality. This research was partially supported by Grant NSh-3003.2008.2 of the Russian Ministry for Science and Education and by RFBR Grants 06-02-17171-a and 07-02-00553-a.

[1] M. Baldo, U. Lombardo, E. E. Saperstein, and M. V. Zverev, Phys. Rep. **391**, 261 (2004).
[2] M. V. Zverev and E. E. Saperstein, Sov. J. Nucl. Phys. **42**, 683 (1985).
[3] M. Baldo, U. Lombardo, E. E. Saperstein, and M. V. Zverev, Nucl. Phys. **A628**, 503 (1998).
[4] M. Baldo, U. Lombardo, E. E. Saperstein, and M. V. Zverev, Phys. Lett. **B459**, 437 (1999).
[5] M. Farine and P. Schuck, Phys. Lett. **B459**, 444 (1999).
[6] M. Baldo, M. Farine, U. Lombardo, E. E. Saperstein, P. Schuck, and M. V. Zverev, Eur. Phys. J. A **18**, 17 (2003).
[7] S. S. Pankratov, M. Baldo, U. Lombardo, E. E. Saperstein, and M. V. Zverev, Nucl. Phys. **A765**, 61 (2006).
[8] S. S. Pankratov, M. Baldo, U. Lombardo, E. E. Saperstein, and M. V. Zverev, Nucl. Phys. **A811**, 127 (2008).
[9] N. Pillet, N. Sandulescu, and P. Schuck, Phys. Rev. C **76**, 024310 (2007).
[10] J.-F. Berger, M. Girod, and D. Gogny, Comput. Phys. Commun. **63**, 365 (1991).
[11] F. Catara, A. Insolia, E. Maglione, and A. Vitturi, Phys. Rev. C **29**, 1091 (1984).
[12] L. Ferreira, R. Liotta, C. H. Dasso, R. A. Broglia, and A. Winther, Nucl. Phys. **A426**, 276 (1984).

[13] G. F. Bertsch and H. Esbensen, Ann. Phys. (NY) **209**, 327 (1991).
[14] K. Hagino, H. Sagawa, J. Carbonell, and P. Schuck, Phys. Rev. Lett. **99**, 022506 (2007).
[15] U. Lombardo and P. Schuck, Phys. Rev. C **63**, 038201 (2001).
[16] S. A. Fayans, S. V. Tolokonnikov, E. L. Trykov, and D. Zawischa, Nucl. Phys. **A676**, 49 (2000).
[17] F. Barranco, R. A. Broglia, G. Colo, G. Gori, E. Vigezzi, and P. F. Bortignon, Eur. Phys. J. A **21**, 57 (2004).
[18] A. V. Avdeenkov and S. P. Kamerdzhiev, JETP Lett. **69**, 715 (1999).
[19] S. Kamerdzhiev and E. E. Saperstein, Eur. Phys. J. A **37**, 333 (2008).